Extrusion melt flow instabilities in long chain branched polyethylenes

Roland Kádár

Chalmers University of Technology, SE 412 58 Gothenburg, Sweden

ABSTRACT

The influence of molecular weight and long chain branching of low density polyethylenes on the onset of extrusion instabilities was investigated in this study. The flow stability was determined via the spectral dynamics from in-situ inline optical imaging as well as pressure fluctuations and preliminary results are here presented.

INTRODUCTION

During polymer melt extrusion processing, extrudates can exhibit surface and volume defects. These defects are known as extrusion melt flow instabilities. Comprehensive reviews on the topic of melt flow instabilities can be found in the works of Denn,[1] Hatzikiriakos and Migler,[2] Larson[3] and Leonov and Prokunin,[4] among others.[5] In the case of linear/short chain branched polymer melts, the main recorded instability types are sharkskin, the stick-slip instability and gross melt fracture,[1,2,6] which have been the focus of most of the scientific research on the subject. However, surface and volume oscillations can additionally occur in long chain branched polymers as well.[5] Overall, a wide variety of flow patterns can be obtained by varying the molecular topology, molecular weight, the polydispersity index (PDI = M_w/M_n where M_w and M_n are the weight and number averaged molecular weights) of the melt, the kinematic conditions, e.g. shear rate, and boundary conditions, i.e. the flow channel material etc.[5] The ensuing patterns can be distinguished by the number of characteristic frequencies present in the recorded patterns via high sensitivity instability detection dies coupled with optical image analysis.[5,7,8] Pressure fluctuations can be linked to extrusion flows exhibiting instabilities, typically limited to the stick-slip and gross melt fracture regimes in conventional melt pressure transducers[7,9] compared to the sensitivity of measurement systems based on piezoelectric transducers capable of detcting fine surface defects, e.g. sharkskin.[10–12] In this framework, the influence of molecular weight and long chain branching of low density polyethylenes (LDPE) on the onset and development of extrusion instabilities was investigated in this study.

EXPERIMENTAL

The extrusion flow stability experimental system, Fig. 1, comprises a Brabender 19/25D single screw extruder equipped with a com-

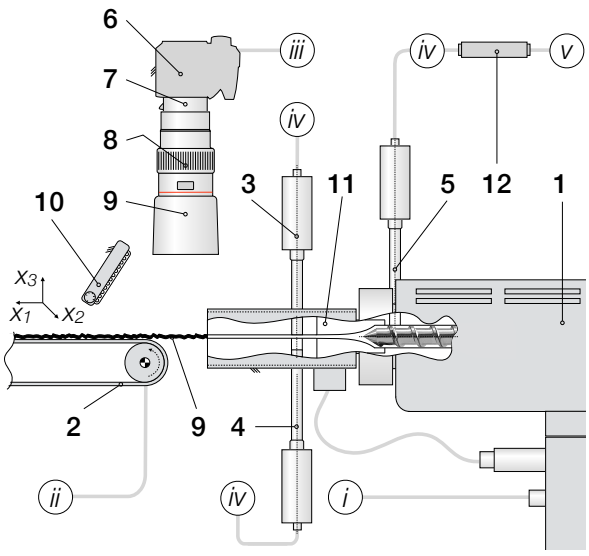

Figure 1. Overview of the experimental extrusion system: (1) Brabender 25/19D single screw extruder, (2) Brabender conveyor belt, (3), (4), (5) melt pressure transducers, (6), (7), (8), (9) camera (10) illumination system, (11) slit die and (12) NI Data acquisition board.

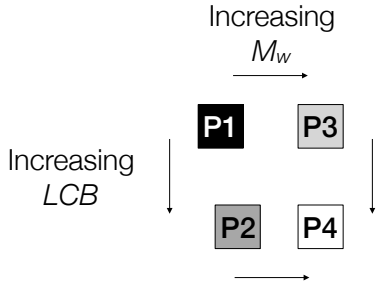

Figure 2. The four low density polyethylenes tested, P1-4, with respect to their molecular weight (M_w) and long chain branching (LCB).

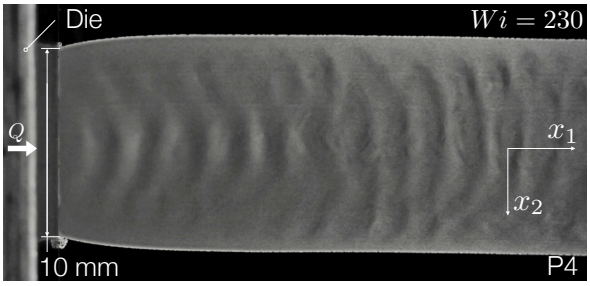

Figure 3. Inline optical extrudate visualization (single frame) of sample P4 at $Wi = 230$ ($\dot{\gamma}_a = 25$ s^{-1}, $n = 65$ rpm).

pression screw (2:1) and a custom slit die ($W \times H \times L = 20 \times 2 \times 100$ mm). The custom die allows for multiple (mechanical) pressure channel measurements including the determination of normal stress differences via the 'hole effect',[5,13] see transducers (3) and (4) in Fig. 1. Terwin 2000 700 bar transducers were used, with transducer (4) flush-mounted for the present study. The pressure data used to evaluate the experiments was acquired using transducer (3). The transducer signals were digitized using a National Instruments data acquisition board and acquired snd oversampled[10,12–14] and using a custom LabVIEW routine.

Four commercial LDPEs (LyondellBasell; P1-4) were compared. The samples allow for the cross-comparison of increasing long chain branching (LCB) at low and high molecular weights M_w, Fig. 2. Samples P1 has the lowest M_w, followed by sample P2 whereas samples P3 and P4 have approximately the same M_w. At the same time, in terms of LCB, the samples are paired as P1, P3 and P2, P4 with the latter pair having higher LCB compared to the former. The rheological characterization of the polymers was performed on an Anton Paar MRC702 TwinDrive equipped with a convection oven (CTD 450TD) and using a 25 mm plate-plate geometry at 140° C.

For the flow stability, a die apparent shear rate ramp rate of $\dot{\gamma}_a = 0.039$ s^{-1} was imposed to insure the same flow history, $\dot{\gamma}_a$ was computed based mass conservation between the barrel/screw zones and the die.[5] This corresponds to a slope in screw speed of $\dot{n} = 0.0017$ s^{-2} (0.1 rpm/s), the lowest allowed by the instrument. A die temperature of 140°C was imposed, low by processing standards but ensuring instabilities are induced early in the shear rate range investigated. The Weissenberg number, Wi, was used as control parameter for flow stability as $Wi = \lambda \dot{\gamma}_a$, where λ is a polymer characteristic relaxation time defined here as the inverse of the angular frequency at the crossing between the dynamic moduli. Inline extrudate optical video recordings were performed at 60 and 200 fps, with spatio-temporal diagrams ((x_1,t) and (x_2,t), see Fig. 3) therefrom created. Simultaneously, in-situ mechanical pressure fluctuations were recorded via transducer (3), Fig. 1. Both the mechanical pressure data and the grey image intensities were then analyzed via Fourier-transformation and compared. The samples were then compared in terms of spectral dynamics of the two signals. Complementary, SEM analysis of the extruded samples was performed. In this publication, a brief outline of the preliminary results is presented.

RESULTS AND DISCUSSION

The rheological characterization (linear viscoelasticity) of the samples tested at processing temperature (140°C) is presented in Fig. 4. The viscosity function follows the variation of M_w as stated. The determined crossing of the dynamic moduli, taken as characteristic polymer relaxation time, were $\lambda_{P1} = 1.51$ s, $\lambda_{P2} = 0.63$ s, $\lambda_{P3} = 0.14$ s and $\lambda_{P4} = 0.11$ s.

The presence of instabilities was detected

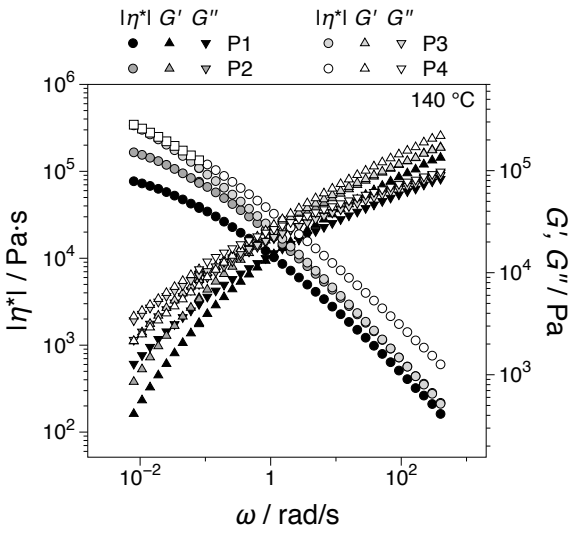

Figure 4. The complex viscosity and dynamic moduli functions for the materials investigated.

for all samples using the image analysis and in-situ mechanical pressure signals, similar to the results of Kádár et al. (2016).[5] As expected, the characteristic instability frequencies at onset are one order of magnitude lower compared to linear / short chain branched polymers, typically $f_{ch} \propto 10^0$ Hz compared to $f_{ch} \propto 10^1$.[5] Two types of instabilities were detected, primary (at the onset of instabilities) having one characteristic pattern frequency, $\#f_{ch} = 1$ and secondary (supercritical) having two characteristic frequencies $\#f_{ch} = 2$, respectively. In the case of the secondary instabilities, a frequency typically a magnitude lower compared to the main characteristic frequency is superimposed on the main frequency. Examples of mechanical pressure, $p(t)$, variation with time and Weissenberg number (upper axis), Wi, with markers at the onset of instabilities are shown in Fig. 5 for P1 and P4. In terms of the onset instabilities, Both increasing M_w and increasing LCB had a stabilizing effect on the onset of instabilities as the onset of instabilities occurred at $Wi_{cr1} = 4$ ($\dot{\gamma}_a = 6.2$ s$^{-}1$, $n = 16$ rpm) for P1, having the lowest M_w and LCB content, whereas $Wi_{cr1} = 29$ ($\dot{\gamma}_a = 3.1$ s$^{-}1$, $n = 8$ rpm) for sample P4, having highest M_w and LCB. The LCB appeared to have a slightly greater influence as $Wi_{cr1} = 13$ ($\dot{\gamma}_a = 1.9$ s$^{-}1$, $n = 5$ rpm) for P3

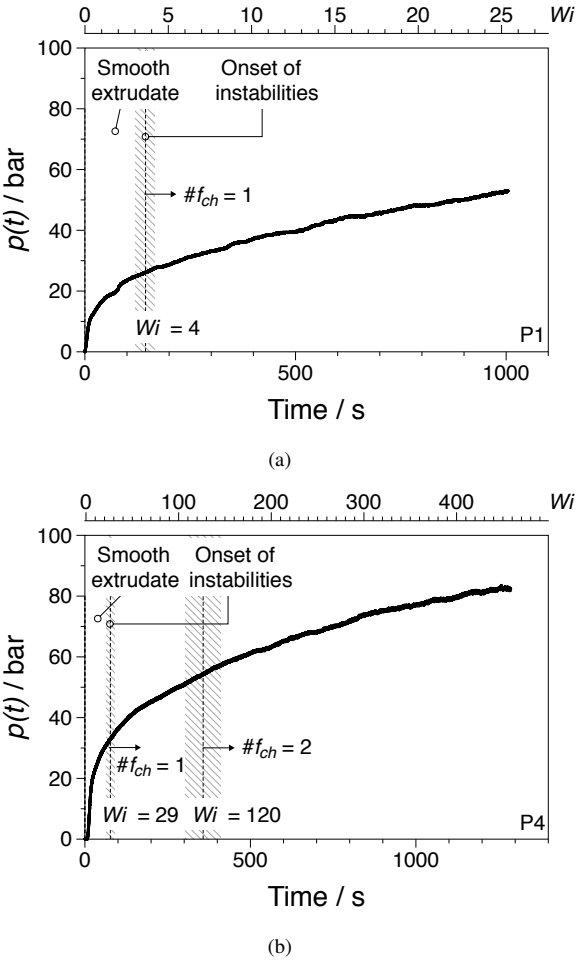

Figure 5. Oversampled time dependent mechanical pressure, $p(t)$ for samples (a) P1 and (b) P4, featuring the onset and development of instabilities.

compared to $Wi_{cr1} = 6$ ($\dot{\gamma}_a = 3.9$ s$^{-}1$, $n = 10$ rpm) for P2. The critical parameters for the onset of instabilities showed approximately 15% error between measurements (hatched regions in Fig. 5). Samples P3 and P4 able to achieve higher Wi numbers in the shear rate range and the temperature investigated are prone to secondary disturbances at $Wi = 80$ ($\dot{\gamma}_a = 11.6$ s$^{-}1$, $n = 30$ rpm) for P3 and $Wi = 120$ ($\dot{\gamma}_a = 12.8$ s^{-1}, $n = 33$ rpm) for P4. In both cases, low frequency surface distortions (ca. $5 \cdot 10^{-2}$ Hz) were detected on the extrudates at onset. However, these initial distortions developed to full volume distortions only for sample P4, in contrast to P3. An example of spatio-temporal dia-

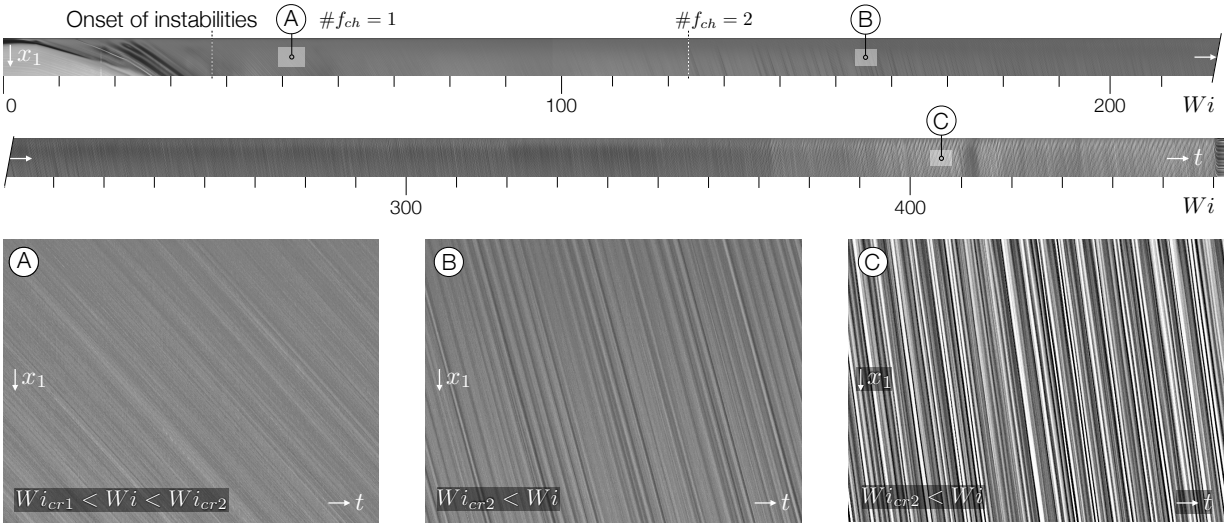

Figure 6. Spatio-temporal (x_1, t) visualization of a complete test for sample P4. The imaging data corresponds to the the pressure data in Fig. 5(b).

gram, (x_2, t), showing the pattern development during extrusion for sample P4 is presented in Fig. 6. In the figure, shaded areas can be detected, starting with $Wi = 120$ (e.g. detail - B), however, they appear fully developed into volume distortions only later (e.g. detail - C). Altogether, the preliminary results point out towards interesting extrusion instability features in long chain branched polyethylenes with respect to their molecular properties, e.g. molecular weight, long chain branching, that deserve further exploration.

ACKNOWLEDGEMENTS

The author is grateful to Dr. Iakovos Vittorias of Basell Polyolefine GmbH, LyondellBasell, for the polymer samples and data thereof.

REFERENCES

1. Denn, M. (2001). "Extrusion instabilities and wall slip". *Annu. Rev. Mech.*, 33, 265–287.

2. Hatzikiriakos, S. and Migler, K., editors (2005). Polymer processing instabilities. Control and understanding. Marcel Dekker.

3. Larson, R.G. (1992). "Instabilities in viscoelastic flows". *Rheol. Acta*, 31, 213–263.

4. Leonov, A. and Prokunin, A. (1994). Nonlinear phenomena in flows of viscoelastic polymer fluids. Chapman & Hall.

5. Kádár, R., Naue, I., and Wilhelm, M. (2016). "First normal stress difference and in-situ spectral dynamics in a high sensitivity extrusion die for capillary rheometry via the 'hole effect"'. *Polymer*, 104, 193–203.

6. Musil, J. and Zatloukal, M. (2014). "Historical review of die drool phenomenon in plastics extrusion". *Polym. Rev.*, 54, 139–184.

7. Naue, I.F., Kádár, R., and Wilhelm, M. (2015). "A new high sensitivity system to detect instabilities during the extrusion of polymer melts". *Macromol. Mater. Eng.*, 300, 1141–1152.

8. Kádár, R., Naue, I.F.C., and Wilhelm, M. (2014). "Simultaneous in-situ analysis of instabilities and first normal stress difference during polymer melt extrusion flows". *Annu. Trans. of the Nordic Rheol. Soc.*, 22, 153–160.

9. den Doelder, J., Koopmans, R., Dees, M., and Mangnus, M. (2005). "Pressure oscillations and periodic extrudate distortions of long-chain branched polyolefins". *J. Rheol.*, 49, 113–126.

10. Palza, H., Naue, I.F.C., and Wilhelm, M. (2009). "In situ pressure fluctuations of polymer melt flow instabilities: Experimental evidence about their origin and dynamics". *Macromol. Rapid Commun.*, 30, 1799–1804.

11. Palza, H., Filipe, S., Naue, I.F.C., and Wilhelm, M. (2010). "Correlation between polyethylene topology and melt flow instabilities by determining in-situ pressure fluctuations and applying advanced data analysis". *Polymer*, 51, 522–534.

12. Ratzsch, K.F., Kádár, R., Naue, I.F.C., and Wilhelm, M. (2013). "A combined NMR relaxometry and surface instability detection system for polymer melt extrusion". *Macromol. Mater. Eng.*, 298, 1124–1132.

13. Teixeira, P.F., Hilliou, L., Covas, J.A., and Maia, J.M. (2013). "Assessing the practical utility of the hole-pressure method for the in-line rheological characterization of polymer melts". *Rheol. Acta*, 52, 661–672.

14. van Dusschoten, D. and Wilhelm, M. (2001). "Increased torque transducer sensitivity via oversampling". *Rheol. Acta*, 40, 395–399.